Computational Studies of Catechol and Water Interactions with Titanium Oxide Nanoparticles

P. C. Redfern,[†] P. Zapol,[†,‡] L. A. Curtiss,*[,†,‡] T. Rajh,[†] and M. C. Thurnauer[†]

Chemistry and Materials Science Divisions, Argonne National Laboratory, Argonne, Illinois 60439

Received: March 24, 2003

The interaction of catechol and water with titanium oxide nanoparticles was investigated using ab initio molecular orbital theory and density functional theory. Hydrogen-terminated TiO_2 clusters were used to model the surface of anatase nanoparticles. The calculations indicate that catechol reacts with a Ti═O defect site on the surface to form a bidentate structure that is favored over dissociative or molecular adsorption on the (101) anatase surface. The dissociative adsorption of catechol at the defect site leads to a much larger red shift in the TiO_2 excitation energy than molecular adsorption on the (101) anatase surface on the basis of ZINDO/S calculations. This is consistent with recent experimental results on small (<2 nm) titania nanoparticles. The calculations on water adsorption indicate that it can also add to the Ti═O double bond site. However, molecular adsorption of water on the (101) anatase surface is more favorable.

I. Introduction

Titanium oxide, TiO_2, is cheap, nontoxic, and photostable but has a wide band gap that limits photocatalytic applications based on solar radiation. The surfaces of anatase nanoparticles were studied by Gao et al.[1] who observed predominantly anatase (101), (010), and (001) surfaces at low pH and (112) and (103) surfaces at high pH. Recently, the optical properties of TiO_2 nanocrystals have been modified by the adsorption of electron-donating ligands such as ascorbic acid.[2] It is believed that the large curvature of small (20-Å) nanoparticles converts octahedral surface sites into undercoordinated corner defects involving Ti═O double bonds, which are reactive toward these ligands and result in bidentate dissociative bonding.[2−4] XANES studies show a decrease in coordination number in going from 500- to 20-Å particles, and EXAFS studies indicate the existence of shorter Ti−O bonds in 20-Å particles (1.79 Å) than in bulk anatase (1.96 Å). The FTIR of ascorbic acid bound to small TiO_2 nanoparticles is consistent with bidentate binding resulting from two ascorbic acid oxygens bonded to a titanium atom. XANES and EXAFS of the ligated species show a return to octahedrally coordinated Ti having bulk anatase geometry.[2] These surface-modified nanoparticles also show a 1.6-eV red shift in the optical spectra (absorption edge at 736 nm vs 380 nm for unmodified TiO_2).[2] Such a large red shift does not occur for ascorbic acid binding to large nanoparticles. Finally, EPR studies suggest a charge-transfer mechanism with the ligand acting as the donor site and the conduction band of TiO_2 acting as the acceptor.[2,5] Interactions of catechol with anatase nanoparticles were observed to show behavior similar to that of ascorbic acid.[6]

There have been theoretical studies[7−14] of molecular interactions on the surfaces of the rutile structure of TiO_2 as well as on the anatase surface of TiO_2.[15−17] The anatase (101) surface was calculated by Vittadini et al.[15,18] to be one of the lowest-energy surfaces of anatase. The adsorption of water on the anatase (101) and (001) surfaces modeled by a periodic two-layer slab was studied by Vittadini et al.[15] using density functional theory within a Car-Parrinello approach with ultrasoft pseudopotentials and the Perdew91 exchange-correlation functional. They found that on the (101) surface molecular adsorption with two hydrogen bonds to neighboring bridging oxygens is preferred over dissociative adsorption at both low and monolayer coverage. The binding energy for the molecular adsorption on this surface was 17 kcal/mol. In contrast, Vittadini et al.[15] found that dissociative adsorption is more favorable than molecular adsorption on the anatase (001) surface. Studies of the molecular adsorption of water on the rutile (110) surface using density functional theory and a cluster model have reported an adsorption energy of 24 kcal/mol,[8] similar to the anatase results. The adsorption of formic acid on the anatase (101) surface has also been studied by Vittadini et al.[19] and was found to result in molecular adsorption. Persson et al.[16] have reported ZINDO/S studies of the interaction of catechol with the (001) anatase surface using cluster models. They found only a small shift (50 nm) in the optical spectra for a dissociative bidentate structure on this surface. This shift was explained by the direct injection

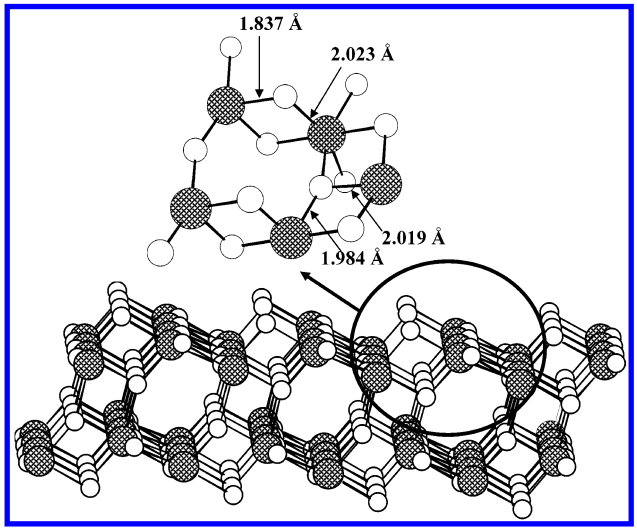

Figure 1. Anatase (101) surface (side and top views)

* Corresponding author. E-mail: curtiss@anl.gov.
† Chemistry Division.
‡ Materials Science Division.

10.1021/jp0303669 CCC: $25.00
Published on Web 09/18/2003

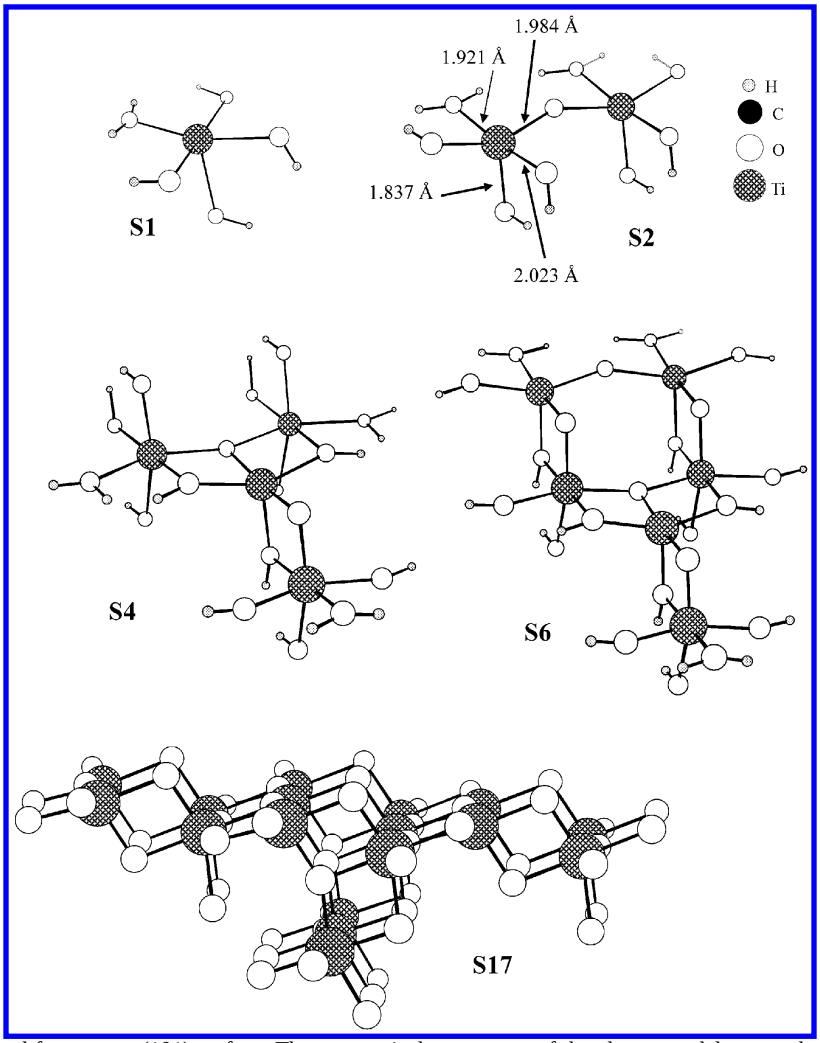

Figure 2. Cluster models used for anatase (101) surface. The geometrical parameters of the cluster models were obtained from a relaxed anatase (101) surface(see text) and kept unchanged throughout the calculations, except where noted.

of an electron from the HOMO on catechol into the LUMO on the titanium dioxide.

The recent experimental studies of Rajh et al.[2] on TiO_2 nanoparticles of ~20 Å have raised several issues that have not been addressed in previous theoretical studies. First, the studies suggest that defect sites present on the surfaces of very small TiO_2 nanoparticles may be very reactive to certain molecules such as catechol and ascorbic acid. Such sites have not been considered in previous studies of anatase surfaces, which have focused on molecular interactions with the (101) surface. Second, Rajh et al. have observed a large optical red shift of about 1.6 eV (360 nm) when catechol and ascorbic acid are adsorbed on their TiO_2 nanoparticles. The work by Lunell et al. on catechol adsorbed on a flat (001) anatase surface is consistent with other experimental studies on anatase surfaces but does not give insight into the large absorption-edge shifts on the surfaces of small nanoparticles studied by Rajh et al.[2]

In this paper, we examine several aspects of water and catechol binding on the anatase (101) surface and on an undercoordinated defect site to address questions raised by the recent experimental studies including (1) the reactivity of the relaxed (101) surface sites versus defect sites and (2) the optical shifts resulting from adsorption at the two types of sites. In section II, we discuss the theoretical methods used in this study and the cluster models employed to represent the adsorption sites. In section III, results for the structures and energies of the molecular adsorption and dissociative adsorption of water and catechol on these clusters are presented. In addition, excitation energies for the different sites calculated using the ZINDO/S method are presented. Conclusions are drawn in section IV.

II. Theoretical Methods

Most of the calculations were performed at the HF/6-31G* and B3LYP/6-31G* levels of theory using the Gaussian 98 computer code.[20] The HF/6-31G* method was used for partial geometry optimizations, and the B3LYP/6-31G* method was used to assess the reaction energies at the HF/6-31G* geometries. Partial geometry optimizations were also done on the small clusters with correlation effects included at the MP2/6-31G* and B3LYP/6-31G* levels. Single-point energies were also calculated with larger basis sets at the B3LYP level. The larger basis sets included 6-31+G(2df,p), 6-311+G(2df,p),[21,22] and the G3MP2Large basis set.[23−25] The 6-31G* basis set used for Ti is from the recently derived set for transition-metal elements[26] and is consistent with the first-row elements (H−F). This basis set is also used in the 6-31+G(2df,p) calculations. The 6-311G basis set in the 6-311+G(2df,p) calculations for the first-row transition metals is based on a Wachter basis set as implemented in Gaussian 98. The 6-311G basis in Gaussian 98 has a different type of contraction scheme than the 6-311G basis sets for the first row (H−F). Thus, we also used the G3MP2Large basis set[25] that has recently been optimized using

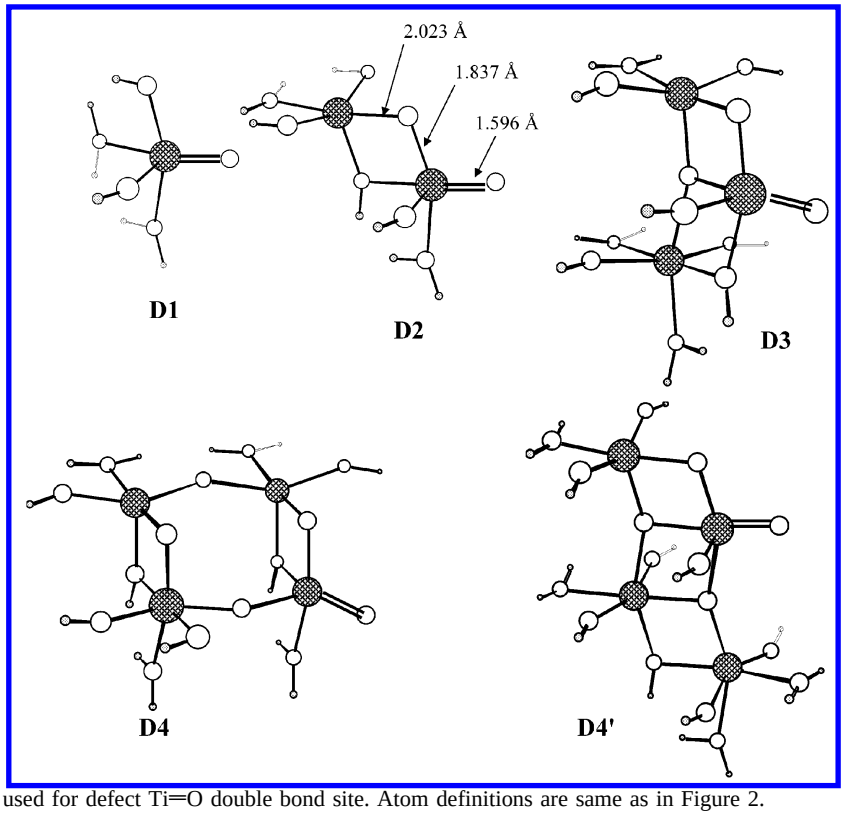

Figure 3. Cluster models used for defect Ti═O double bond site. Atom definitions are same as in Figure 2.

TABLE 1: Summary of Calculations on Interactions of H_2O on Cluster Models of the Anatase (101) Surface

			reaction energy, kcal/mol			
TiO_2 cluster	adsorbate structure	reaction[a]	HF/6-31G* //HF/6-31G*	B3LYP/6-31G* //HF/6-31G*	B3LYP/6-31G* //B3LYP/6-31G*[b]	B3LYP /6-311+G(2df,p) //HF/6-31G*[c]
TiO_5H_6	mol. complex	**S1** + H_2O → **W1**	−30.1	−29.0	−29.5(−31.1)	−21.3
$Ti_2O_9H_{10}$	mol. complex	**S2** + H_2O → **W3**	−30.2	−29.8		−21.6(−20.9)
$Ti_4O_{17}H_{18}$	mol. complex	**S4** + H_2O → **W5**	−32.4	−27.8		
$Ti_6O_{22}H_{20}$	mol. complex	**S6** + H_2O → **W7**	−29.0	−26.4		
	mol. complex	**S6** + H_2O → **W8**	−29.3	−27.1		
TiO_5H_6	dissoc. adsorp.	**S1** + H_2O → **W2**	−13.3	−11.2	−11.7(−11.5)	−3.6
$Ti_2O_9H_{10}$	dissoc. adsorp.	**S2** + H_2O → **W4**	−18.4	−16.1		−8.4 (−7.7)
$Ti_4O_{17}H_{18}$	dissoc. adsorp.	**S4** + H_2O → **W6**	−30.2	−19.4		
$Ti_6O_{22}H_{20}$	dissoc. adsorp.	**S6** + H_2O → **W9**	−27.5	−19.8		
	dissoc. adsorp.	**S6** + H_2O → **W10**	−23.5	−15.6		

[a] See Figure 2 for TiO_2 cluster structures (**Sn**) and Figure 4 for the water−TiO_2 structures (**W3**−**W10**). [b] Values in parentheses are from MP2/6-31G*//MP2/6-31G* calculations. [c] Values in parentheses are from B3LYP/G3MP2Large//HF/6-31G* calculations.

a contraction for the third row (K−Kr) that is consistent with the first (Li−Ne) and second (Na−Ar) rows.

The cluster models for adsorption sites were obtained from a relaxed anatase (101) surface[15,18] structure shown in Figure 1 and were kept unchanged throughout the calculations, except where noted. Hydrogen saturators were used on oxygens with dangling bonds so that the clusters were closed shell with neutral charge. The choice of where to put hydrogen saturators is somewhat arbitrary, so a series of different-sized clusters were examined to determine the effect on the results. In some cases, the binding energies are quite sensitive to the placement of the hydrogen saturators. Two different types of adsorption sites were examined for water and catechol. The first corresponds to a titanium atom coordinated to five oxygens at the (101) surface. Clusters modeling this site including 1 (**S1**), 2 (**S2**), 4 (**S4**), and 6 (**S6**) titanium atoms are shown in Figure 2. Also shown in Figure 2 is a 17-atom cluster (**S17**) that was used to embed the smaller clusters in a larger cluster for single-point calculations of excitation energies. The second site corresponds to a defect site that contains a titanium atom coordinated to five oxygen atoms, one of these corresponding to a Ti═O double bond. This is similar to the defect sites suggested by Rajh et al.[2] Clusters modeling this site including 1 (**D1**), 2 (**D2**), 3 (**D3**), and 4 (**D4** and **D4′**) titanium atoms are shown in Figure 3. We considered two possible four-titanium-atom clusters with Ti═O bonds, **D4** and **D4′**. Partial optimizations of the adsorbate−surface structures were carried out, including (1) the intramolecular water or catechol parameters, (2) the Ti═O bond length for the defect sites, and (3) the intermolecular geometrical parameters. These optimizations are referred to as "//" in the tables. The OH distances on the anatase portion of the clusters were fixed at 0.95 Å. In some cases, limited relaxation of the (101) surface structure near the adsorption site was allowed. Catechol was chosen for this study because it is very similar to ascorbic acid but smaller for calculations.

Excitation energies were calculated with the configuration interaction ZINDO/S method[27] in HyperChem.[28]

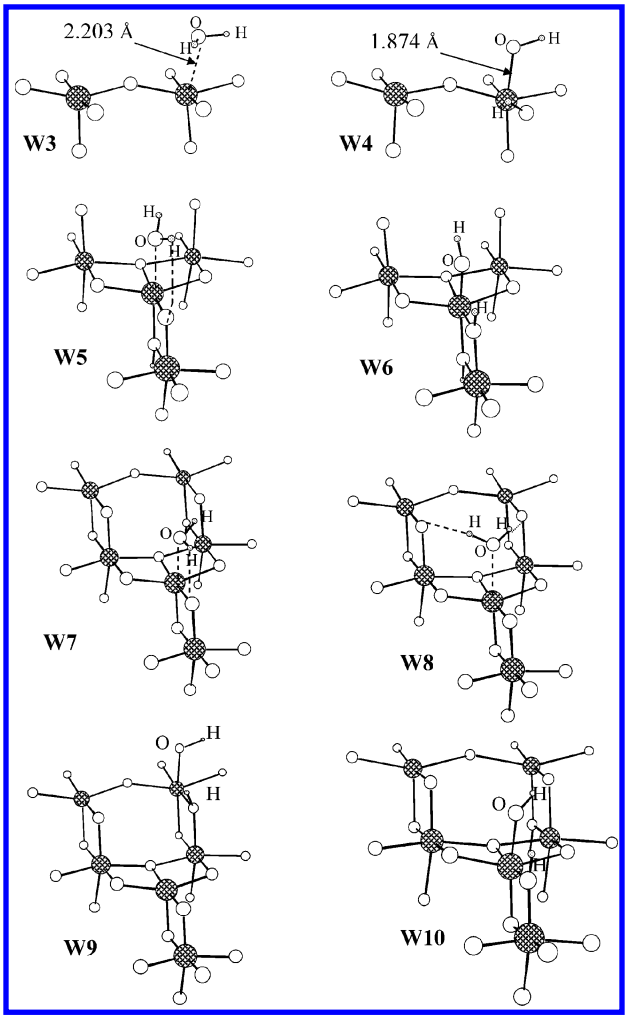

Figure 4. Molecular adsorption and dissociative adsorption of H_2O on cluster models of anatase (101) surface. Terminal hydrogens not shown. Atom definitions are same as in Figure 2.

III. Results and Discussion

A. Water Adsorption. The calculations on the interaction of an H_2O molecule with five coordinated titanium (101) surface sites using the **S1**, **S2**, **S4**, and **S6** frozen cluster models are summarized in Table 1. Molecular adsorption structures for H_2O on the **S2**, **S4**, and **S6** clusters (**W3**, **W5**, **W7**, **W8**) are shown in Figure 4. This Figure also contains the dissociative H_2O structures on the **S2**, **S4**, and **S6** clusters (**W4**, **W6**, **W9**, and **W10**). The calculations for the reaction of an H_2O molecule with a defect site having a Ti═O double bond using the **D1**, **D2**, **D3**, and **D4** cluster models are summarized in Table 2. Dissociative H_2O structures on the **D4** and **D6** clusters (**W13**, **W14**) are shown in Figure 5.

The relaxation of the TiO_2 surface near the interaction site may affect the adsorption energies. We have investigated this possibility by performing calculations with local surface relaxation on the molecular adsorption structure for H_2O on the **S4** cluster (**W5**) and for the dissociative H_2O structure on the **S4** clusters (**W6**). The partial surface relaxation was done by allowing five of the cluster atoms nearest the interaction site in **S4** (Ti1, O1, O2, O3, O4, O5 in Figure 6) to relax their positions in the geometry optimization in calculations of the free cluster and in the complex. The optimizations were done at the HF/6-31G* level, followed by single-point energy calculations at the B3LYP/6-31G* level. The results of these calculations are summarized in Table 3. They show very little change in the adsorption energies when the surface atoms near the interaction site are allowed to relax. The H_2O molecular adsorption energy changes by only 1.4 kcal/mol, from −27.8 to −26.4 kcal/mol, and the H_2O dissociative energy also changes by only 1.4 kcal/mol, from −19.4 to −20.8 kcal/mol. Thus, surface relaxation in our cluster models leads to only small changes in the adsorption energies of water. These results should also apply to the adsorption energies calculated at higher levels of theory.

The results for molecular and dissociative adsorption in Tables 1 and 2 show a dependence on the level of theory and cluster size. The structures based on clusters with one and two titanium atoms indicate that the 6-31G* basis tends to overestimate the binding energies by 5−10 kcal/mol compared to the larger 6-311+G(2df,p) and G3MP2Large basis sets. For example, increasing the basis set from 6-31G* to 6-311+G(2df,p) changes the B3LYP molecular adsorption energy from −29.8 to −21.6 kcal/mol for the **W3** complex. The G3MP2Large basis set gives an adsorption energy of −20.9 kcal/mol, which is nearly the same as that from 6-311+G(2df,p). This suggests that 6-311+G(2df,p) is adequate. The dependence on cluster size in Tables 1 and 2 suggests that the adsorption energies are in most cases approximately converged in clusters containing two titanium atoms. The results in Table 1 also indicate that the HF/6-31G* and B3LYP/6-31G* geometries give similar reaction energies for the one-titanium-atom clusters, indicating that Hartree−Fock geometries should be reasonable. On the basis of the above results, the B3LYP/6-311G(2df,p) energies for the clusters containing two titanium atoms (**S2** and **D2**) are used in the following discussion of the water adsorption structures.

The molecular adsorption of water occurs with the formation of a van der Waals bond between the oxygen of water and a five-coordinated titanium atom as in **W3** (Figure 4). In some cases, a hydrogen from water also forms hydrogen bonds with an oxygen of the TiO_2 lattice as in **W5**, **W7**, and **W8** (Figure 4). The dissociative state involves the breaking of one O−H bond in water that adds a hydrogen to a surface oxygen and an O−H to a five-coordinated titanium atom, as shown in structures **W4**, **W6**, **W9**, and **W10** in Figure 4. The results in Table 1 indicate that molecular adsorption on the (101) surface is more favorable than dissociative adsorption. The molecular adsorption energy at the five-coordinated titanium (101) surface sites on the **S2** cluster is −21.6 kcal/mol compared to a dissociative energy of only −8.4 kcal/mol (B3LYP/6-311+G(2df,p).

The adsorption energies in Table 1 calculated at our highest level of theory are consistent with previous studies on water adsorption on anatase[15] and rutile[7] surfaces. The molecular adsorption energy of −21.6 kcal/mol (−20.2 kcal/mol with relaxation effects extrapolated from the **W5** cluster included) is in reasonable agreement with a previous density functional study[15] with ultrasoft pseudopotentials that gave −17 kcal/mol for water adsorption on the anatase (101) surface. The dissociative adsorption energy of −8.4 kcal/mol is in reasonable agreement with the density functional pseudopotential[15] value of −6.9 kcal/mol.

The dissociative addition of water at the edge site involves the breaking of one OH bond in water that adds a hydrogen to the oxygen in Ti═O and an OH to the titanium of this site, as shown in structures **W13** and **W14** in Figure 5. The results in Table 2 indicate that the dissociative energy for the addition of water at the Ti═O site of the **D2** cluster is −18.2 kcal/mol (B3LYP/6-311+G(2df,p)). Thus, the edge site is significantly more reactive toward the dissociative addition of water than the (101) surface, which has a reaction energy of −8.4 kcal/mol, but is still slightly less stable than the molecular adsorption

TABLE 2: Summary of Calculations on Interactions of H_2O and Catechol at the Defect Ti═O Double Bond Site

			reaction energy, kcal/mol		
TiO_2 cluster	adsorbate structure	reaction[a]	HF/6-31G*//HF/6-31G*	B3LYP/6-31G*//HF/6-31G*	B3LYP/6-311+G(2df,p)//HF/6-31G*[b]
TiO_5H_6	dissoc. adsorp.	**D1** + H_2O → **W11**	−27.6	−24.8	−20.2 (−20.0) [−19.7]
$Ti_2O_8H_8$	dissoc. adsorp.	**D2** + H_2O → **W12**	−26.1	−21.9	−18.2 (−18.3) [−17.7]
$Ti_3O_{12}H_{12}$	dissoc. adsorp.	**D3** + H_2O → **W13**	−25.1	−21.4	
$Ti_4O_{15}H_{14}$	dissoc. adsorp.	**D4** + H_2O → **W14**	−31.7	−25.4	
TiO_5H_6	bidendate	**D1** + catechol → **C7** + H_2O	−27.2	−25.3	−24.3 (−25.0) [−24.6]
$Ti_2O_8H_8$	bidendate	**D2** + catechol → **C8** + H_2O	−27.5	−23.8	−24.7 (−25.3) [−24.8]
$Ti_3O_{12}H_{12}$	bidendate	**D3** + catechol → **C9** + H_2O	−31.6	−28.4	
$Ti_4O_{15}H_{14}$	bidendate	**D4** + catechol → **C10** + H_2O	−32.2	−26.2	
$Ti_4O_{16}H_{16}$	bidendate	**D4′** + catechol → **C11** + H_2O	−35.4	−31.0	[−30.1]

[a] See Figure 3 for TiO_2 cluster defect structures (**Dn**) and Figure 5 for water−TiO_2 (**W13**−**W14**) and catechol−TiO_2 (**C9**−**C11**) structures. [b] Values in parentheses are from B3LYP/G3MP2Large//HF/6-31G* calculations. Values in square brackets are from B3LYP/6-31+G(2df,p)//HF/6-31G calculations.

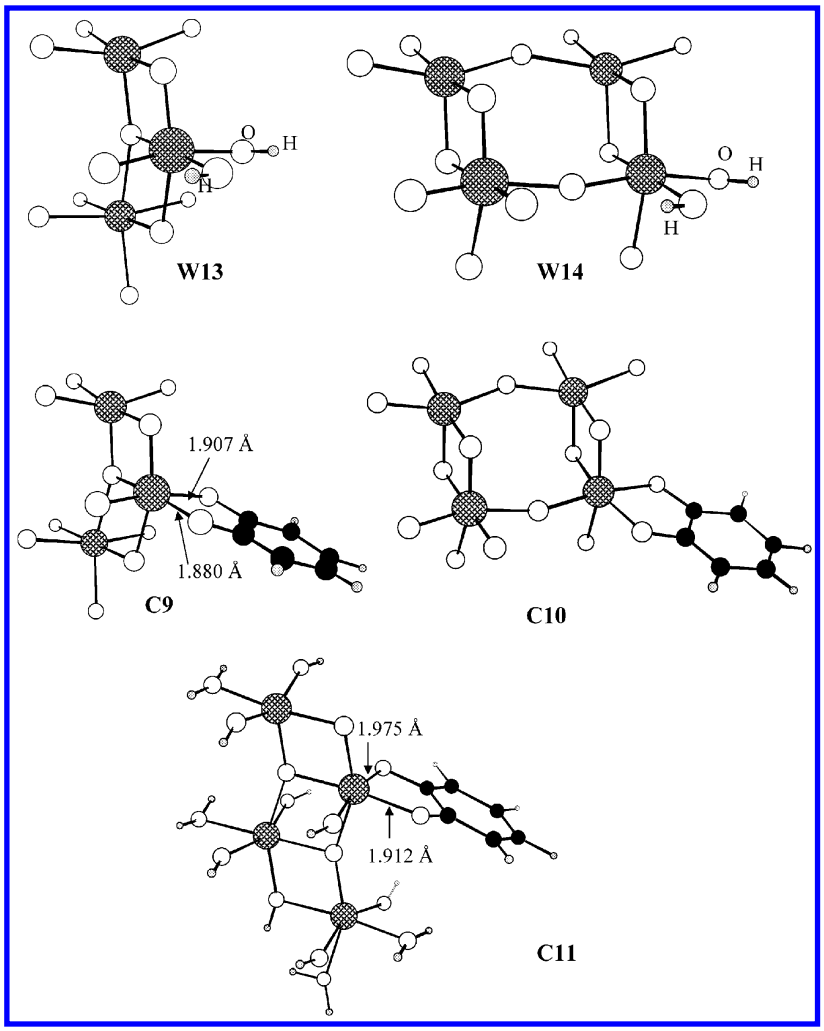

Figure 5. Dissociative addition of water and dissociative bidentate adsorption of catechol at a defect Ti═O double bond site.Terminal hydrogens not shown. Atom definitions are same as in Figure 2.

of water on the (101) surface. We have not examined reaction barriers for the dissociative reactions that will also influence the importance of these processes.

B. Catechol Adsorption. Molecules having OH groups such as catechol may adsorb on the surface of a TiO_2 nanoparticle by molecular adsorption or by dissociative adsorption. In the former process, a van der Waals complex with hydrogen bonds is formed. In dissociative adsorption on the (101) surface, a hydrogen atom dissociates from one of the catechol OH groups and attaches to a bridging oxygen on the surface, and the remaining catechol oxygen bonds to a five-coordinate surface titanium atom forming a monodentate structure. On the (101) surface, the dissociation of two hydrogens from the catechol can lead to the formation of a bidentate bridging structure with two surface titanium atoms. At a defect T═O site, there can be H_2O elimination resulting in a bidentate structure with two chemical bonds from catechol to a surface titanium.

The calculations on the interaction of catechol with a single five-coordinated titanium atom at (101) surface sites using the **S1**, **S2**, and **S4** cluster models are summarized in Table 4.

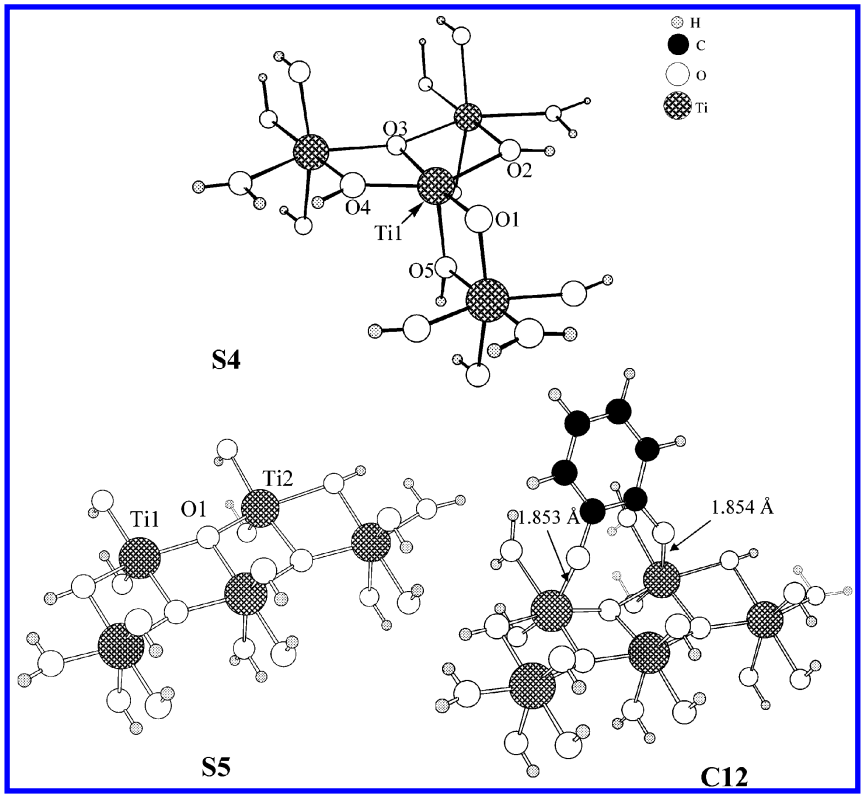

Figure 6. Cluster model used for investigating the effect of (101) surface relaxation at interaction site for a 4 Ti cluster and a 5 Ti atom cluster. Also shown is the bridging structure for catechol when it is dissociatively adsorbed on two titanium atoms The numbered atoms are relaxed.

TABLE 3: Effect of Cluster Relaxation near the Interaction Site (B3LYP/6-31G*//HF/6-31G* results)

			B3LYP/6-31G*//HF/6-31G* reaction energy, kcal/mol		B3LYP /6-31+G(2df,p)[d]
TiO_2 cluster	adsorbate structure	reaction[a]	frozen TiO_2 cluster	partially relaxed TiO_2 cluster[b]	partially relaxed TiO_2 cluster[d]
$Ti_4O_{17}H_{18}$	mol. complex	**S4** + H_2O → **W5**	−27.8	−26.4	
$Ti_4O_{17}H_{18}$	dissoc. adsorp.	**S4** + H_2O → **W6**	−19.4	−20.8	
$Ti_4O_{17}H_{18}$	mol. complex	**S4** + catechol → **C5**	−29.0	−25.9	(−18.5)
$Ti_4O_{17}H_{18}$	monodentate	**S4** + catechol → **C6**	−26.9	−28.4	(−19.4)
$Ti_5O_{20}H_{20}$	bridging[c]	**S5** + catechol → **C12**	1.8	−23.8	−17.4

[a] See Figure 2 for TiO_2 cluster structures (**Sn**), Figure 4 for the water−TiO_2 structures (**W5**, **W6**), and Figure 7 for the catechol−TiO_2 structures (**C5**, **C6**). [b] In the partially relaxed structure, six atoms (Ti1, O1, O2, O3, O4, O5 in Figure 6**)** of **S4** near the interaction site are allowed to relax their positions in the geometry optimization in calculations of the free cluster and in the complex. For **S5**, three atoms (Ti1, Ti2, O1 in Figure 6) are allowed to relax. All other atoms in the cluster are held fixed as in the rigid cluster model (Figure 2). In the **S5** cluster for the bridging site, three atoms (Ti1, Ti2, O1) in Figure 6 are allowed to relax. [c] Bidentate structure with dissociatively adsorbed catechol bridging two titanium atoms (Figure 6). [d] At the HF/6-31G* geometry of the partially relaxed structure. Values in parentheses are extrapolated from B3LYP/6-311+G(2df,p) energies for **S2** in Table 4.

TABLE 4: Summary of Calculations on Interactions of Catechol on Cluster Models of the Anatase (101) Surface

			reaction energy, kcal/mol		
TiO_2 cluster	adsorbate structure	reaction[a]	HF/6-31G* //HF/6-31G*	B3LYP/6-31G* //HF/6-31G*	B3LYP /6-311+G(2df,p) //HF/6-31G*[b]
TiO_5H_6	mol. complex	**S1** + catechol → **C1**	−26.8	−24.7	−17.6 (−17.2)
$Ti_2O_9H_{10}$	mol. complex	**S2** + catechol → **C3**	−31.4	−28.8	−21.4 (−20.9)
$Ti_4O_{17}H_{18}$	mol. complex	**S4** + catechol → **C5**	−35.2	−29.0	[−21.6]
TiO_5H_6	monodentate	**S1** + catechol → **C2**	−23.1	−23.3	−12.8 (−12.9)
$Ti_2O_9H_{10}$	monodentate	**S2** + catechol → **C4**	−24.9	−25.1	−16.0
$Ti_4O_{17}H_{18}$	monodentate	**S4** + catechol → **C6**	−34.3	−26.9	[−17.9]

[a] See Figure 2 for TiO_2 cluster structures (**Sn**) and Figure 7 for some representative catechol−TiO_2 (**C3**−**C6**) structures. [b] Values in parentheses are from B3LYP/G3MP2L//HF/6-31G* calculations. Values in brackets are extrapolated from B3LYP/6-311+G(2df,p) energies for **S2**.

Molecular adsorption structures for catechol on the **S2** and **S4** clusters (**C3**, **C5**) are shown in Figure 7. This Figure also contains the dissociative catechol structure on the **S2** and **S4** clusters (**C4**, **C6)**. We were unable to find any stable bidentate structures on the (101) surface involving one titanium atom because it would require seven coordination of the resulting titanium site. The calculations for the reaction of a catechol molecule with a defect site having a Ti═O double bond using

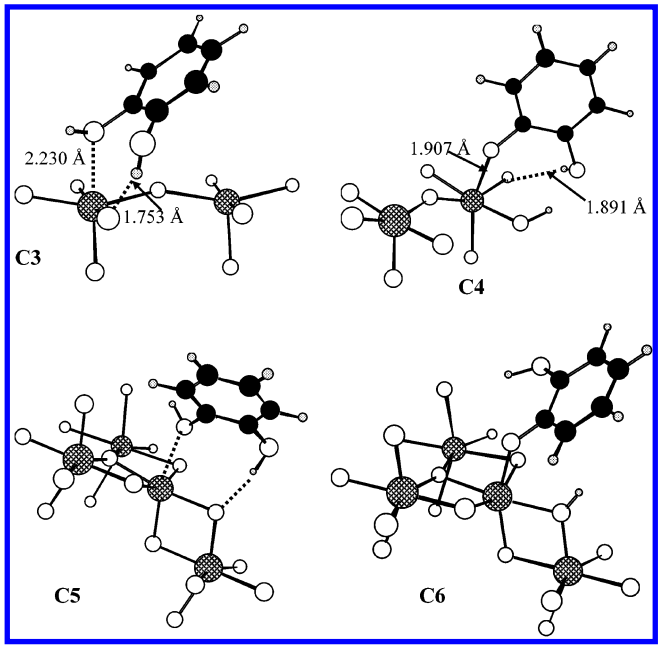

Figure 7. Monodentate dissociative and molecular adsorption of catechol on cluster models of anatase (101) surface.Terminal hydrogens not shown. Atom definitions are same as in Figure 2.

the **D1**, **D2**, **D3**, **D4**, and **D4′** cluster models are summarized in Table 2. Dissociative catechol structures on the **D3**, **D4**, and **D4′** clusters (**C9**, **C10**, **C11**) are shown in Figure 5. These are all bidentate structures. A bridging bidentate structure on the (101) surface was also investigated and is shown in Figure 6 as **C12**.

For the adsorption of catechol on the (101) surface, the results in Table 4 indicate that the 6-31G* basis tends to overestimate the binding energies by 5−10 kcal/mol compared to the larger basis sets whereas for the adsorption at the edge site the 6-31G* basis set gives results similar to those of the larger basis sets (Table 2). The reason for this difference is unclear, but all three large basis sets used in Table 2 for the defect site give similar results. In addition, there is more dependence on cluster size with the reaction energies tending to increase with increasing cluster size.

The molecular adsorption of catechol on a five-coordinated titanium (101) surface site occurs with the formation of two van der Waals bonds (O−H- - -O and O- - -Ti) as shown in structures **C3** and **C5** in Figure 7. The dissociative state on the (101) surface involves breaking one O−H bond and adding a hydrogen to a surface oxygen as shown in structures **C4** and **C6** in Figure 7. The B3LYP/6-311+G(2df,p) results in Table 4 indicate that molecular adsorption on the (101) surface is more favorable by about 4−5 kcal/mol than dissociative adsorption. However, if one considers surface relaxation effects similar to that for H_2O (Table 3), then the reaction energies of the molecular and monodentate structures are approximately the same (ca. −19 kcal/mol). There is a small amount of electron transfer (∼0.02e) from the nearest titanium atom to catechol upon the formation of the monodentate and molecular complexes.

Another possible adsorbate structure for catechol on the (101) surface involves a bridging structure. Persson et al.[16] have reported ZINDO/S studies of the interaction of catechol with an anatase surface using a frozen cluster model for anatase. They assumed a bridging structure on an anatase surface with the two catechol oxygens interacting with two surface Ti atoms.

TABLE 5: Excitation Energies[a] (eV) of TiO_2 Clusters and Catechol−TiO_2 Clusters

TiO_2 cluster	site	adsorbate structure	absorption	shift
$Ti_2O_8H_8$ (**D2**)			4.60	
$Ti_2O_9H_{10}$ (**S2**)			5.23	
$Ti_3O_{12}H_{12}$ (**D3**)			4.14	
$Ti_4O_{15}H_{14}$ (**D4**)			4.15	
$Ti_4O_{16}H_{16}$ (**D4′**)			4.75	
$Ti_4O_{17}H_{18}$ (**S4**)			5.42	
$Ti_5O_{20}H_{20}$ (**S5**)			5.79	
$Ti_{17}O_{55}H_{42}$ (**S17**)			4.75	
$Ti_2O_9H_{10}$	101	mol. complex (**C3**)	5.16	−0.06
$Ti_4O_{17}H_{18}$	101	mol. complex (**C5**)	5.61	0.19
$Ti_2O_9H_{10}$	101	monodentate (**C4**)	4.27	−0.96
$Ti_4O_{17}H_{18}$	101	monodentate (**C6**)	4.92	−0.50
$Ti_2O_8H_8$	Ti═O	bidentate (**C8**)	3.42	−1.17
$Ti_3O_{12}H_{12}$	Ti═O	bidentate (**C9**)	2.39	−1.75
$Ti_4O_{15}H_{14}$	Ti═O	bidentate (**C10**)	3.39	−0.76
$Ti_4O_{16}H_{16}$	Ti═O	bidentate (**C11**)	2.93	−1.82
$Ti_5O_{20}H_{20}$	101	bridging bidentate (**C12**)	4.76	−1.03
$Ti_{17}O_{55}H_{42}$[b]	101	mol. complex	4.38	−0.37
$Ti_{17}O_{55}H_{42}$[b]	101	monodentate	3.55	−1.20
$Ti_{17}O_{55}H_{42}$[b]	Ti═O	bidentate	3.52	−1.23

[a] Calculated at the HF/6-31G* geometries of the adsorbates. All calculations were made with (20 × 20) CI; energies are for the first excited state corresponding to catechol to the TiO_2 cluster. With the exception of **C3**, **C5**, **C4**, and **C6**, this is the first excited state overall. In the latter cases, the first excited states are catechol to catechol (see text). [b] Based on embedding the 4 Ti atom cluster in a 17 Ti atom cluster; for the bidentate structure, the **C10** cluster was used.

They did not perform any geometry optimizations of this structure. Using unrelaxed clusters, we were unable to find a stable catechol structure that bridges two Ti atoms because bidendate bridging between two Ti atoms is strained (Table 3). However, when the partial relaxation of the surface is allowed, there is significant stabilization. The results for the frozen and relaxed clusters are given in Table 3 for a $Ti_5O_{20}H_{20}$ cluster. With relaxation, the dissociative bidentate bridging structure has a dissociative reaction energy of −17.4 kcal/mol at the B3LYP/6-31+G(2df,p) level, similar to that of the monodentate and molecular structures on the (101) surface.

The dissociative addition of catechol at the edge site (Ti═O) results in a bidentate structure as shown in structures **C9**−**C11** in Figure 5. It involves the loss of H_2O. The results in Table 2 indicate that the dissociative energy for the addition of catechol at the Ti═O site is −24.8 kcal/mol and −30.1 kcal/mol for the **D2** and **D4′** clusters, respectively (B3LYP/6-31+G(2df,p)). Thus, the edge site is significantly more reactive toward catechol than either the molecular adsorption or dissociative addition on the (101) surface. This is probably due to the formation of the two chemical bonds to one titanium at a defect site. There is significant electron transfer from titanium to catechol upon the formation of this bidentate structure as the net Mulliken charge on the nearest titanium increases from 1.76 to 1.96.

Water and catechol may compete for a defect site. Water can react with a Ti═O double bond to form $Ti(OH)_2$ (**W13** and **W14**), and catechol can react with Ti═O to form a bidentate structure (**C9**−**C11**). The results in Table 2 indicate that catechol forms a more stable structure than water with the edge site.

C. Optical Spectra of TiO_2−Catechol Complexes. Experimental results[2] indicate a shift to longer wavelengths in the optical spectra when molecules such as catechol or ascorbic acid bind to small TiO_2 nanoparticles. We calculated singlet

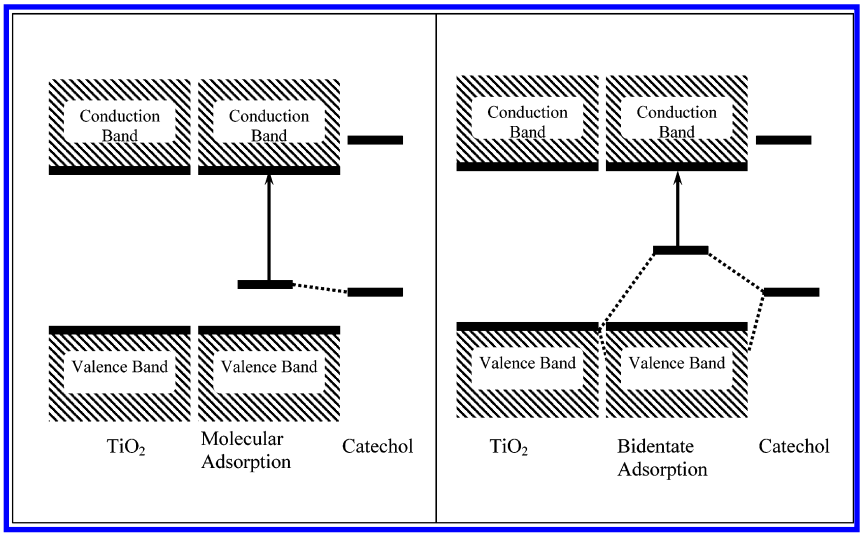

Figure 8. Schematic illustration of electronic structure of catechol adsorbed on TiO_2 nanoparticles molecularly and dissociatively (bidentate).

excitation energies of the TiO_2−catechol complexes from section III.B using ZINDO/S. We also embedded the Ti_4 complexes into a large Ti_{17} cluster (**S17** in Figure 2) to take into account long-range effects. All of the results are summarized in Table 5 and are for the first catechol to TiO_2 excitation. In most cases, this is the lowest excitation, although in some of the smaller clusters catechol to catechol is the lowest because the TiO_2 LUMO is too high in small clusters. The calculation of excitation energies involving nanoparticles can be properly described only with a cluster large enough to represent the band structure of the nanoparticle involved. The strong dependence of the excitation energies on the cluster size in Table 5 is evidence of the need for large clusters for excitation energy calculations. However, there are trends from the smaller clusters that help explain the experimental observation of a large red shift.

The calculated excitation energies of the free TiO_2 clusters in Table 5 used for modeling catechol adsorption range from 4.1 to 5.4 eV. These values are larger than the experimental result of 3.45 eV for TiO_2 nanoparticles. This could be due to the small clusters being used to model the nanoparticle and/or the use of the ZINDO/S method. The calculated excitation energies of the molecular complexes of catechol (**C3**, **C5**) with clusters containing two and four titanium atoms exhibit small shifts (0.1−0.2 eV). Monodentate adsorption on the anatase (101) surface represented by clusters containing two and four titanium atoms (**C4**, **C6**) leads to red shifts of 0.5−1.0 eV. The bridging bidentate structure (**C12**) on the (101) surface has a shift of 1.0 eV. Bidentate adsorption at the defect site in the cluster models (**C8**−**C11**) leads to red shifts of 0.8−1.8 eV. In the $Ti_{17}O_{55}H_{42}$ cluster, molecular adsorption on the (101) surface leads to a red shift of 0.4 eV whereas dissociative monodentate adsorption on the (101) surface and bidentate adsorption at the defect site lead to red shifts of 1.2 eV.

Thus, the excitation energy results in Table 5 indicate that a van der Waals-type interaction with the surface such as in a molecular complex will lead to small shifts in the optical spectra (<0.5 eV) and that dissociative adsorption such as monodentate or bidentate leads to larger shifts (>1 eV). These results suggest that the observed shift of 0.4 eV[29] for adsorbates on large nanoparticles is due to molecular adsorption on a (101) surface because the monodentate structure would give a larger shift. The theoretical results suggest that the experimental shift of 1.6 eV on smaller nanoparticles[2] is due to dissociative adsorption at the defect site. As discussed in the previous section, the reaction energy for the bidentate structure at the defect site is significantly larger than that for the three structures considered on the (101) surface. Although we cannot make a definite conclusion as to which of the three structures exist on the (101) surface because of the similarity in their reaction energies, the absence of a significant red shift would indicate that the molecular complex is predominant. The results for the water complexes are not given here, but they indicate only small shifts.

An examination of the molecular orbital (MO) coefficients of the orbitals involved in the excitation of the adsorbate−TiO_2 complex indicates that the electron is excited from an MO primarily associated with catechol carbon atoms to an MO delocalized on some of the titanium atoms. This occurs for both molecular and dissociative catechol adsorption, giving rise to a photoinjection mechanism of excitation.[16] The energy levels of the adsorbate−TiO_2 clusters are illustrated schematically in Figure 8 for both the molecular complex and the bidentate adsorbate. There is a larger red shift of the absorption edge for the bidentate or monodentate compared to that for the molecular complex because of stronger interaction between catechol and titanium oxide energy levels for the former type of interaction. Evidence for the stronger interaction comes from an examination of the molecular orbitals, which show a stronger mixing of catechol and TiO_2 orbitals in the HOMO of the bidentate and monodentate structures compared to that in the molecular complex. Also, the bidentate and monodentate structures have $Ti-O_{catechol}$ distances of 1.9−2.0 Å, which are shorter than in the molecular complex (2.2−2.3 Å) and are closer to the bulk Ti−O distances. Therefore, the HOMO−LUMO gap is smaller for the shorter bonds than for the van der Waals bonds, causing a larger red shift.

IV. Conclusions

The interaction of catechol and water with titanium oxide nanoparticles was investigated using ab initio molecular orbital theory and density functional theory. Hydrogen-terminated TiO_2 clusters were used to model the surface of titanium dioxide nanoparticles. The following conclusions can be drawn from this study.

(1) These calculations indicate that catechol reacts with a Ti=O defect site on the surface to form a bidentate structure with an adsorption energy of about 25−30 kcal/mol and support experimental evidence for this type of structure on small TiO_2

nanoparticles. The catechol bidentate structure is more favorable than dissociative or molecular adsorption on the (101) anatase surface.

(2) The adsorption of catechol at the defect site leads to a larger red shift in the TiO_2 excitation energy than molecular adsorption on the (101) anatase surface. This is consistent with recent experimental results on observations of a large red shift for the adsorption of catechol and ascorbic acid on small (20-Å) TiO_2 nanoparticles and is probably due to the formation of two Ti−O bonds at the defect site. The excitation occurs from a molecular orbital primarily associated with catechol carbon atoms to a molecular orbital delocalized on some of the titanium atoms and corresponds to charge transfer from the catechol to the TiO_2 cluster.

(3) The calculations on water adsorption indicate that it can also add to Ti═O double bonds at corner defect sites on TiO_2 nanoparticles. Molecular adsorption on the (101) anatase surface is more favorable than dissociative adsorption.

There were several approximations made in this study that may affect the conclusions, including the limited relaxation of the TiO_2 surface near the adsorption site, the structure of the edge or corner sites, the use of the Hartree−Fock level for geometry optimizations of the clusters with two or more Ti atoms, and the size of the clusters used for the calculation of the excitation energies. The relaxation question has been addressed in several cases and does not seem to be very significant unless the adsorbate is interacting with two titanium atoms. These issues will be addressed in more detailed studies in the future.

Acknowledgment. This work was supported by the U.S. Department of Energy, Division of Chemical Sciences, under contract no. W-31-109-ENG-38 and the Northwestern Institute for Environmental Catalysis.

References and Notes

(1) Gao, Y.; Elder S. A. *Mater. Lett.* **2000**, *44*, 228.

(2) Rajh, T.; Nedeljkovic, J. M.; Chen, L. X.; Poluektov, O.; Thurnauer, M. C. *J. Phys. Chem. B* **1999**, *103*, 3519.

(3) Chen, L. X.; Rajh, T.; Wang, Z. Thurnauer, M. C. *J. Phys. Chem. B* **1997**, *101*, 10688.

(4) Chen, L. X.; Rajh, T.; Jager, J.; Nedeljkovic, J.; Thurnauer, M. C. *J. Synchron Radiat.* **1999**, *6*, 445.

(5) Rajh, T.; Poluektov, O.; Dubinski, A. A.; Wiederrecht, G.; Thurnauer, M. C.; Trifunac, A. D. *Chem. Phys. Lett.* **2001**, *344*, 31.

(6) Rajh, T. Unpublished results.

(7) Stefanovich, E. V.; Truong, T. N. *Chem. Phys. Lett.* **1999**, *299*, 623.

(8) Casarin, M.; Maccato, C.; Vittadini, A. *Appl. Surf. Sci.* **1999**, *142*, 196.

(9) Bredow, T. *Int. J. Quantum Chem.* **1999**, *75*, 127.

(10) Rittner, F.; Fink, R.; Boddenberg., B.; Staemmler, V. *Phys. Rev. B* **1998**, *57*, 4160.

(11) Lindan, P. J. D.; Harrison, N. M.; Gillan, M. J. *Phys. Rev. Lett.* **1998**, *80*, 762.

(12) Persson, P.; Stashans, A.; Bergstrom, R.; Lunell, S. *Int. J. Quantum Chem.* **1998**, *70*, 1055.

(13) Persson, P.; Lunell, S.; Bruhwiler, P. A.; Schnadt, J.; Sodergren, S.; O'Shea, J. N.; Karis, O.; Siegbahn, H.; Martensson, N.; Bassler, M.; Pattehy, L. *J. Chem. Phys.* **2000**, *112*, 3945.

(14) Patthey, L.; Persson, P.; Westermark, K., Vayssieres, L.; Stanhans, A.; Petersson, A.; Bruhwiler, P. A.; Siegbahn, H.; Lunell, S.; Martensson, N. *J. Chem. Phys.* **1999** *110*, 5913.

(15) Vittadini, A.; Selloni, A.; Rotzinger, F. P.; Grätzel, M. *Phys. Rev. Lett.* **1998**, *81*, 2954.

(16) Persson, P.; Bergström, R.; Lunell, S. *J. Phys. Chem. B* **2000**, *104*, 10348.

(17) Bredow, T.; Jug, K. *J. Phys. Chem.* **1995**, *99*, 285.

(18) Lazerri, M.; Vittadini, A.; Selloni. A. *Phys. Rev. B* **2001**, *63*, 155409.

(19) Vittadini, A.; Selloni, A.; Rotzinger, F. P.; Grätzel, M. *J. Phys. Chem. B* **2000**, *104*, 1300.

(20) Frisch, M. J.; Trucks, G. W.; Schlegel, H. B.; Scuseria, G. E.; Robb, M. A.; Cheeseman, J. R.; Zakrzewski, V. G.; Montgomery, J. A., Jr.; Stratmann, R. E.; Burant, J. C.; Dapprich, S.; Millam, J. M.; Daniels, A. D.; Kudin, K. N.; Strain, M. C.; Farkas, O.; Tomasi, J.; Barone, V.; Cossi, M.; Cammi, R.; Mennucci, B.; Pomelli, C.; Adamo, C.; Clifford, S.; Ochterski, J.; Petersson, G. A.; Ayala, P. Y.; Cui, Q.; Morokuma, K.; Malick, D. K.; Rabuck, A. D.; Raghavachari, K.; Foresman, J. B.; Cioslowski, J.; Ortiz, J. V.; Stefanov, B. B.; Liu, G.; Liashenko, A.; Piskorz, P.; Komaromi, I.; Gomperts, R.; Martin, R. L.; Fox, D. J.; Keith, T.; Al-Laham, M. A.; Peng, C. Y.; Nanayakkara, A.; Gonzalez, C.; Challacombe, M.; Gill, P. M. W.; Johnson, B. G.; Chen, W.; Wong, M. W.; Andres, J. L.; Head-Gordon, M.; Replogle, E. S.; Pople, J. A. *Gaussian 98*; Gaussian, Inc.: Pittsburgh, PA, 1998.

(21) Hehre, W. J.; Radom, L.; Pople, J. A.; Schleyer, P. v. R. *Ab Initio Molecular Orbital Theory*; John Wiley: New York, 1987.

(22) The 6-311+G(2df,p) basis for titanium is Wachter's basis set (Wachters, A. J. H. *J. Chem. Phys.* **1970**, *52*, 1033) as implemented in Gaussian 98.[20]

(23) Curtiss, L.A.; Redfern, P. C.; Raghavachari, K.; Rassolov, V.; Pople, J. A. *J. Chem. Phys.* **1999**, *110*, 4703.

(24) (a) Curtiss, L. A.; Redfern, P. C.; Rassolov, V.; Kedziora, G.; Pople, J. A. *J. Chem. Phys.* **2001**, *114*, 9287. (b) Curtiss, L. A.; Raghavachari, K. Redfern, P. C.; Rassolov, V.; Pople, J. A. *J. Chem. Phys.* **1998**, *109*, 7764.

(25) Rassolov, V.; Redfern, P.; Curtiss, L. A.; Pople, J. A. To be submitted for publication.

(26) (a) Rassolov, V.; Pople, J. A.; Ratner, M. A.; Windus, T. L. *J. Chem. Phys.* **1998**, *109*, 1223. (b) Rassolov, V.; Ratner, M. A.; Pople, J. A.; Redfern, P. C.; Curtiss, L. A. *J. Comput. Chem.* **2001**, *22*, 976.

(27) Zerner, M. C. *Rev. Comput. Chem.* **1991**, *2*, 313.

(28) *HyperChem 6.0*; Hypercube, Inc.: Gainesville, FL.

(29) (a) Moser, J.; Punchihewa, S.; Infelta, P. P.; Graetzel, M. *Langmuir* **1991**, *7*, 3012 (b) Rodriquez, R.; Blesa, M. A.; Regazzoni, A. E. *Colloid Interfaces Sci.* **1996**, *177*, 122.